九州大学大学院総合理工学府報告
第 45 巻 1 号 25-30 頁 令和 5 年 9 月

Engineering Sciences Reports, Kyushu University
Vol. 45, No. 1, pp. 25-30, SEP, 2023

Branching Ratios of Recombination and Neutralization Reactions in the Positive ion–Negative Ion Reactions of Kr^+ and Xe^+ with $C_6F_5Br^-$ and $C_6F_5CF_3^-$ in the Flowing Afterglow

Masaharu TSUJI,[*1,2†] Hiroaki ISHIMI,[*3] Keiko UTO,[*1]
Jun-Ichiro HAYASHI[*1] and Takeshi TSUJI[*4]
[†]E-mail of corresponding author: tsuji@cm.kyushu-u.ac.jp

(Received June 2, 2023, accepted June 13, 2023)

The positive ion–negative ion reactions of Kr^+ and Xe^+ with $C_6F_5Br^-$ and $C_6F_5CF_3^-$ have been spectroscopically studied in the He flowing afterglow. The branching ratios of recombination and neutralization reactions leading to RgX* excimers and excited Rg* atoms (Rg = Kr, Xe, X = Br, F), respectively, were determined to be 0.14:0.86 and 1.00:0.00 for the $Kr^+/C_6F_5Br^-$ and $Xe^+/C_6F_5Br^-$ reactions and 0.00:1.00 for both the $Kr^+/C_6F_5CF_3^-$ and $Xe^+/C_6F_5CF_3^-$ reactions. It was concluded that electron affinities of target molecules and dissociation energies of $C_6F_5X^-$ leading to X^- play a significant role in determining the branching ratio of ion–ion recombination and neutralization reactions.

Key words: *Ion–ion reaction, Flowing afterglow, Emission spectroscopy, Kr^+, Xe^+, $C_6F_5Br^-$, $C_6F_5CF_3^-$ Recombination reaction, Neutralization reaction, Branching ratio, KrBr* excimer, XeBr* excimer, Excited rare gas atoms*

1. Introduction

Because of the strong, long-range Coulomb attractive force between the positive and negative ions, ion–ion mutual recombination reactions are characterized by large cross sections, as much as 10,000 Å^2, at low energies.1,2) Therefore, ion–ion recombination reactions are an important loss process of ions in natural and man-made plasmas involving positive and negative ions. In most cases, the reaction is highly exothermic, so the products may be electronically excited or even dissociated. The main aim of previous studies was to determine the cross sections or reaction rate constants.3-8) Little work has been carried out on the product-state distributions in the ion–ion reactions.

In order to obtain product-state distributions, we have previously made optical spectroscopic studies on the ion–ion reactions between rare gas cations (Rg^+) and such negative ions as SF_6^- and $C_6F_5X^-$ (X = F, Cl) using a flowing-afterglow apparatus.9-17) We determined the branching ratios of recombination reaction leading to RgX* excimer and neutralization reaction leading to excited Rg* atoms. The branching ratios between recombination and neutralization reactions were 0.001:0.999, 0.00:1.00, 0.69:0.31, and 0.89:0.11 for the $Kr^+/C_6F_6^-$, $Xe^+/C_6F_6^-$, $Kr^+/C_6F_5Cl^-$, and $Xe^+/C_6F_5Cl^-$ reactions, respectively.11,16)

In this study, ion–ion reactions of $Kr^+(^2P_{1/2,3/2})$ and $Xe^+(^2P_{1/2,3/2})$ with $C_6F_5Br^-$ and $C_6F_5CF_3^-$ are spectroscopically studied in the He flowing afterglow. The branching ratios of recombination and neutralization reactions leading to RgX* excimers and excited Rg* atoms (Rg = Kr, Xe), respectively, are determined.

$$
\begin{aligned}
&Rg^+ + C_6F_5X^- \ (X = Br,\ CF_3) \\
&\quad \rightarrow RgX^* + C_6F_5 \ \text{(recombination)}, \qquad (1a) \\
&\quad \rightarrow Rg^* + C_6F_5X \ \text{(neutralization)}. \qquad (1b)
\end{aligned}
$$

Results obtained are compared with our previous data for the $Rg^+/C_6F_5X^-$ (X = F, Cl)

---

*1 Institute for Materials Chemistry and Engineering, and Research and Education Center of Green Technology

*2 Department of Molecular Science and Technology

*3 Department of Molecular Science and Technology, Graduate Student

*4 Department of Materials Science, Shimane University reactions.[11,16]

2. Experimental

2.1 Chemicals

Gaseous and liquid samples used in this study were obtained from Japanese chemical companies: He (purity >99.9999%, Taiyo Sanso), Kr (99.995%, Nippon Sanso), Xe (99.99%, Nippon Sanso), C_6F_5Br (Kishida Kagaku, 97%), and $C_6F_5CF_3$ (Kishida Kagaku, 98%). These samples were used without further purification.

2.2 Apparatus and experimental procedures

The flowing-afterglow apparatus used in this study was identical with that reported previously.[16,17] A mixture of $He(2^3S)$, He^+, and He_2^+ was generated by a microwave discharge of high purity He gas in a He flowing afterglow. He^+ and He_2^+ ions in the discharge flow were removed by using a pair of ion-collector grids placed between the discharge section and the reaction zone. A small amount of Kr or Xe gas was added to the He flow 10 cm downstream from the center of microwave discharge. Positive $Kr^+(^2P_{1/2,3/2})$ or $Xe^+(^2P_{1/2,3/2})$ ion were formed by the $He(2^3S)/Kr$ or $He(2^3S)/Xe$ Penning ionization.

$$He(2^3S) + Kr \rightarrow Kr^+(^2P_{1/2,3/2}) + He + e^-. \quad (2)$$
$$(k_2 = 9.94 \times 10^{-11}\ cm^3\ s^{-1}\ [Ref.\ 18])$$

$$He(2^3S) + Xe \rightarrow Xe^+(^2P_{1/2,3/2}) + He + e^-. \quad (3)$$
$$(k_3 = 1.24 \times 10^{-10}\ cm^3\ s^{-1}\ [Ref.\ 18])$$

Further 10 cm downstream from the Kr or Xe gas inlet, an electron attachment gas, C_6F_5Br or $C_6F_5CF_3$, was added, where negative $C_6F_5Br^-$ or $C_6F_5CF_3^-$ ion was formed as major products by a fast electron attachment to these two gases.

$$C_6F_5Br + e^- \rightarrow C_6F_5Br^-\ (\geq 97\%), \quad (4a)$$
$$\rightarrow Br^- + C_6F_5\ (\leq 3\%). \quad (4b)$$
$$(k_{4a} + k_{4b} = 8.3 \times 10^{-8}\ cm^3\ s^{-1}\ [Ref.\ 19])$$

$$C_6F_5CF_3 + e^- \rightarrow C_6F_5CF_3^-. \quad (5)$$
$$(k_5 = 2.42 \times 10^{-7}\ cm^3\ s^{-1}\ [Ref.\ 20])$$

The partial pressures in the reaction zone were 1.0 Torr (1 Torr = 133.33 Pa) for He, 5–40 mTorr for Kr or Xe, and 3–5 mTorr for C_6F_5Br and $C_6F_5CF_3$. A small amount of Br^- anions is formed by a dissociative electron attachment to C_6F_5Br (4b). We previously found that the following three-body recombination reaction occurs at a relatively high He buffer gas pressures of 2–10 Torr in the same flowing-afterglow apparatus.[21]

$$Xe^+(^2P_{1/2,3/2}) + Br^- + He$$
$$\rightarrow XeBr(B,C,D) + He, \quad (6a)$$
$$\rightarrow Br^* + Xe + He. \quad (6b)$$

To suppress above three-body reaction, He buffer gas pressure was maintained at a relatively low pressure of 1.0 Torr in this study.

The emission, observed around the C_6F_5Br or $C_6F_5CF_3$ gas inlet, was dispersed in the 120–840 nm region with McPherson 218 and Spex 1250M monochromators.

We used ionization potentials of Kr and Xe, electron affinities of C_6F_5Br or $C_6F_5CF_3$, dissociation energy of $D(C_6F_5–Br)$, excitation energies of excimers and rare gas atoms reported in Refs. 22–29 for the calculations of energetics in each reaction. To be best of our knowledge, $D(C_6F_5CF_2–F)$ and $D(F–C_6F_4CF_3)$ values are unknown. The $D(C_6F_5CF_2–F)$ value was estimated by using an average value between $D(CF_3–F)$ and $D(CF_3CF_2–F)$, whereas the $D(F–C_6F_4CF_3)$ value was assumed to be the same as that of $D(F–C_6F_5)$.

3. Results and Discussion

3.1 Branching ratios of RgX* and Rg* in the $Kr^+/C_6F_5Br^-$ and $Xe^+/C_6F_5Br^-$ reactions

Figure 1(a) shows a typical emission spectrum resulting from the $Kr^+/C_6F_5Br^-$ reaction. A strong Kr atomic line due to the $Kr(5s[3/2] \rightarrow 4p^6\ ^1S_0)$ transition is observed at 124 nm. In addition, three transitions of KrBr* excimer are observed in the 170–250 nm region.

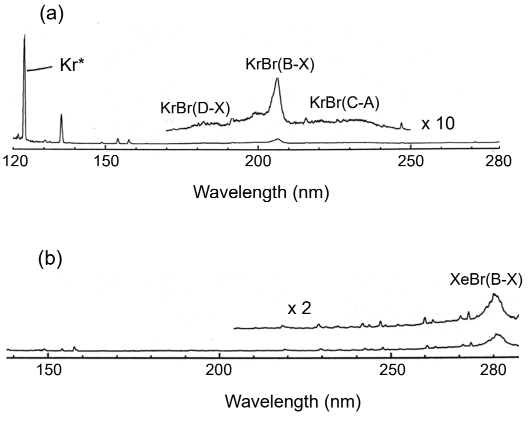

Fig. 1. Emission spectra resulting from the (a) $Kr^+/C_6F_5Br^-$ and (b) $Xe^+/C_6F_5Br^-$ reactions.

KrBr* excimer bands consist of the strong B(1/2)–X(1/2) transition in the 180–210 nm region and the weak broad C(3/2)–A(3/2) transition in the 210–250 nm region. The D(1/2)–X(1/2) transition is observed as a very weak shoulder band of the B–X transition in the 170–190 nm region, The energetics for the formation of KrBr(B,C,D) from the $\mathrm{Kr^+/C_6F_5Br^-}$ reaction is as follows:

$$\begin{aligned}&\mathrm{Kr^+ + C_6F_5Br^-}\\&\quad\rightarrow \mathrm{KrBr(B) + C_6F_5} + 3.5\ \mathrm{eV}, &&\text{(7a)}\\&\quad\rightarrow \mathrm{KrBr(C) + C_6F_5} + 3.5\ \mathrm{eV}, &&\text{(7b)}\\&\quad\rightarrow \mathrm{KrBr(D) + C_6F_5} + 2.8\ \mathrm{eV}. &&\text{(7c)}\end{aligned}$$

All processes are highly exothermic, which are energetically allowed.

Possible mechanisms for the formation of $\mathrm{Kr}(5s[3/2]_1)$ atoms are direct neutralization (8a), neutralization involving radiative cascade from higher energy Kr* states (8b), and predissociation of highly vibrationally excited KrBr** states (8c).

$$\begin{aligned}&\mathrm{Kr^+ + C_6F_5Br^-}\\&\quad\rightarrow \mathrm{Kr}(5s[3/2]_1) + \mathrm{C_6F_5Br} + 2.8\ \mathrm{eV}, &&\text{(8a)}\\&\quad\rightarrow \mathrm{Kr^* + C_6F_5Br},\\&\qquad\downarrow h\nu\ \text{(cascade)}\\&\quad\mathrm{Kr}(5s[3/2]_1) + \mathrm{C_6F_5Br}, &&\text{(8b)}\\&\quad\rightarrow \mathrm{KrBr^{**} + C_6F_5},\\&\qquad\downarrow \text{(predissociation)}\\&\quad\mathrm{Kr}(5s[3/2]_1) + \mathrm{Br + C_6F_5} - 0.58\ \mathrm{eV}. &&\text{(8c)}\end{aligned}$$

Since predissociation process (8c) is endoergic, this process is energetically excluded from possible mechanisms at thermal energy (≈300 K). When emission spectrum in the 400–800 nm region was observed to examine the contribution of the radiative cascade from the upper Kr* states to the $\mathrm{Kr}(5s[3/2]_1)$ state (8b), no Kr* lines were observed. It was therefore concluded that the contribution of process (8b) is negligible and that only direct neutralization process (8a) is responsible for the formation of $\mathrm{Kr}(5s[3/2]_1)$.

Based on above results, both recombination reaction leading to KrBr(B,C,D) (7a)–(7c) and neutralization process (8a) occur competitively in the $\mathrm{Kr^+/C_6F_5Br^-}$ reaction. The branching ratio of processes (7a)–(7c) and (8a) was determined to be 0.14:0.86 by measuring the total intensities of KrBr* and Kr* emissions.

Figure 1(b) shows a typical emission spectrum resulting from the $\mathrm{Xe^+/C_6F_5Br^-}$ reaction in the 140–285 nm region. The B(1/2)–X(1/2) transition of XeBr* with a long tail band degrading to blue is identified in the 250–285 nm region. Although a Xe line due to the $\mathrm{Xe}(6s[3/2]_1 \rightarrow 5p^6\ {}^1S_0)$ was observed at 147 nm in the $\mathrm{Xe^+/C_6F_5Cl^-}$ reaction,[16] it was not found in the $\mathrm{Xe^+/C_6F_5Br^-}$ reaction. The energetics for the formation of XeBr(B) and $\mathrm{Xe}(6s[3/2]_1)$ from the $\mathrm{Xe^+/C_6F_5Br^-}$ reaction is as follows:

$$\begin{aligned}&\mathrm{Xe^+ + C_6F_5Br^-}\\&\quad\rightarrow \mathrm{XeBr(B) + C_6F_5} + 3.2\ \mathrm{eV}, &&\text{(9a)}\\&\quad\rightarrow \mathrm{Xe}(6s[3/2]_1) + \mathrm{C_6F_5Br} + 2.5\ \mathrm{eV}. &&\text{(9b)}\end{aligned}$$

Both processes (9a) and (9b) are energetically allowed. On the basis of spectroscopic data, the branching ratio of (9a):(9b) was found to be 1.00:0.00.

3.2 Branching ratios of RgX* and Rg* in the $\mathrm{Kr^+/C_6F_5CF_3^-}$ and $\mathrm{Xe^+/C_6F_5CF_3^-}$ reactions

Figures 2(a) and 2(b) show emission spectra resulting from the $\mathrm{Kr^+/C_6F_5CF_3^-}$ and $\mathrm{Xe^+/C_6F_5CF_3^-}$ reactions, respectively. A strong $\mathrm{Kr}(5s[3/2]_1 \rightarrow 4p^6\ {}^1S_0)$ line is observed at 124 nm in Fig. 2(a), whereas a strong $\mathrm{Xe}(6s[3/2]_1 \rightarrow 5p^6\ {}^1S_0)$ line is observed at 147 nm in Fig. 2(b).

Possible formation mechanisms of $\mathrm{Kr}(5s[3/2]_1)$ and $\mathrm{Xe}(6s[3/2]_1)$ atoms are direct neutralization (10a) and (11a), neutralization involving radiative cascade from higher energy Kr* and Xe* states (10b) and (11b), and predissociation of highly vibrationally excited KrF** and XeF** states (10c), (10d), (11c), and (11d).

$$\begin{aligned}&\mathrm{Kr^+ + C_6F_5CF_3^-}\\&\quad\rightarrow \mathrm{Kr}(5s[3/2]_1) + \mathrm{C_6F_5CF_3} + 3.1\ \mathrm{eV}, &&\text{(10a)}\\&\quad\rightarrow \mathrm{Kr^* + C_6F_5CF_3},\\&\qquad\downarrow h\nu\ \text{(cascade)}\\&\quad\mathrm{Kr}(5s[3/2]_1) + \mathrm{C_6F_5CF_3}, &&\text{(10b)}\\&\quad\rightarrow \mathrm{KrF^{**} + C_6F_5CF_2}\ \text{or}\ \mathrm{C_6F_4CF_3},\\&\qquad\downarrow \text{(predissociation)}\\&\quad\mathrm{Kr}(5s[3/2]_1) + \mathrm{F + C_6F_5CF_2} - 2.5\ \mathrm{eV}, &&\text{(10c)}\\&\quad\mathrm{Kr}(5s[3/2]_1) + \mathrm{F + C_6F_4CF_3} - 1.9\ \mathrm{eV}. &&\text{(10d)}\end{aligned}$$

$$\begin{aligned}&\mathrm{Xe^+ + C_6F_5CF_3^-}\\&\quad\rightarrow \mathrm{Xe}(6s[3/2]_1) + \mathrm{C_6F_5CF_3} + 2.8\ \mathrm{eV}, &&\text{(11a)}\\&\quad\rightarrow \mathrm{Xe^* + C_6F_5CF_3},\\&\qquad\downarrow h\nu\ \text{(cascade)}\\&\quad\mathrm{Xe}(6s[3/2]_1) + \mathrm{C_6F_5CF_3}, &&\text{(11b)}\\&\quad\rightarrow \mathrm{XeF^{**} + C_6F_5CF_2}\ \text{or}\ \mathrm{C_6F_4CF_3},\\&\qquad\downarrow \text{(predissociation)}\\&\quad\mathrm{Xe}(6s[3/2]_1) + \mathrm{F + C_6F_5CF_2} - 2.8\ \mathrm{eV}, &&\text{(11c)}\\&\quad\mathrm{Xe}(6s[3/2]_1) + \mathrm{F + C_6F_4CF_3} - 2.2\ \mathrm{eV}. &&\text{(11d)}\end{aligned}$$

Since predissociation processes (10c), (10d),

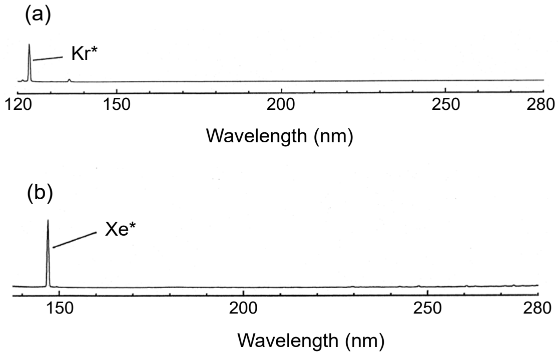

Fig. 2. Emission spectra resulting from the (a) $Kr^+/C_6F_5CF_3^-$ and (b) $Xe^+/C_6F_5CF_3^-$ reactions.

(11c), and (11d) are endoergic, they are energetically excluded from possible mechanisms. In order to examine the contribution of radiative cascade from upper Kr* and Xe* states, processes (10b) and (11b), emission spectra in the 280–800 nm region were measured. The absence of Kr* and Xe* from upper states in the UV and visible region show that these radiative cascade processes are unimportant. Thus, we concluded that direct neutralization reactions (10a) and (11a) are responsible for the formation of Kr($5s[3/2]_1$) and Xe($6s[3/2]_1$).

It is known that KrF(B–X,D–X,C–A) and XeF(B–X,D–X,C–A) excimer emissions are observed in the 150–400 and 200–450 nm region, respectively.[9,30,31] It should be noted that KrF(B–X,D–X,C–A) and XeF(B–X,D–X,C–A) emissions were not observed in the $Kr^+/C_6F_5CF_3^-$ and $Xe^+/C_6F_5CF_3^-$ reaction, even though they are energetically accessible.

$Kr^+ + C_6F_5CF_3^-$

$\rightarrow KrF(B) + C_6F_5CF_2 + 2.3\ eV,$ (12a)

$\rightarrow KrF(B) + C_6F_4CF_3 + 2.9\ eV,$ (12b)

$\rightarrow KrF(C) + C_6F_5CF_2 + 2.3\ eV,$ (12c)

$\rightarrow KrF(C) + C_6F_4CF_3 + 2.8\ eV,$ (12d)

$\rightarrow KrF(D) + C_6F_5CF_2 + 1.6\ eV,$ (12e)

$\rightarrow KrF(D) + C_6F_4CF_3 + 2.2\ eV.$ (12f)

$Xe^+ + C_6F_5CF_3^-$

$\rightarrow XeF(B) + C_6F_5CF_2 + 2.1\ eV,$ (13a)

$\rightarrow XeF(B) + C_6F_4CF_3 + 2.6\ eV,$ (13b)

$\rightarrow XeF(C) + C_6F_5CF_2 + 2.0\ eV,$ (13c)

$\rightarrow XeF(C) + C_6F_4CF_3 + 2.5\ eV,$ (13d)

$\rightarrow XeF(D) + C_6F_5CF_2 + 0.7\ eV,$ (13e)

$\rightarrow XeF(D) + C_6F_4CF_3 + 1.2\ eV.$ (13f)

Thus, it was found that the branching ratios of processes (12a–12f):(10a) and (13a–13f):(11a) are 0.00:1.00 for both reactions.

In Table 1 are summarized the branching ratios of RgX* excimers and Rg* atoms in the reactions of Kr^+ and Xe^+ with $C_6F_5Br^-$ and $C_6F_5CF_3^-$. For comparison, corresponding data for $C_6F_6^-$ and $C_6F_5Cl^-$ are also given.[11,16] Although both $Rg^+(^2P_{1/2})$ and $Rg^+(^2P_{3/2})$ components are formed by Penning ionization (2) and (3), the lower $Rg^+(^2P_{3/2})$ state is expected to be major component in the present experiments as reported previously.[16]

Table 1. Branching ratios of RgX* and Rg* in the reactions of Rg^+ (Rg = Kr and Xe) with $C_6F_5X^-$ (X=F, Cl, Br, and CF_3).

Reaction		KrF(B,C,D)	KrCl(B,C,D)	KrBr(B,CD)	Kr*		
					$5s[3/2]_1$	$5p[3/2]_2$	$5p[5/2]_3$
$Kr^+/C_6F_6^-$	Ref. 11	0.001			0.000	0.454	0.545
$Kr^+/C_6F_5Cl^-$	Ref. 16	0.00	0.69		0.31	0.00	0.00
$Kr^+/C_6F_5Br^-$	This work	0.00		0.14	0.86		
$Kr^+/C_6F_5CF_3^-$	This work	0.00			1.00		

Reaction		XeF(B,C,D)	XeCl(B,C,D)	XeBr(B,C,D)	Xe*	
					$6s[3/2]_1$	$6p[1/2]_0$
$Xe^+/C_6F_6^-$	Ref. 11	0.00			0.00	1.00
$Xe^+/C_6F_5Cl^-$	Ref. 16	0.00	0.89		0.11	0.00
$Xe^+/C_6F_5Br^-$	This work			1.00	0.00	
$Xe^+/C_6F_5CF_3^-$	This work	0.00			1.00	

3.3 Reaction mechanisms for the formation of RgX* and Rg* in the reactions of Rg^+ with $C_6F_5Cl^-$, and $C_6F_5CF_3^-$

We reported that the electron affinity of target molecules and the dissociation energy of C_6F_5–X leading to X^- anion would be principal factor in assessing the branching ratio of the two channels.[11,16] The electron affinities of C_6F_5X provide energies required for an electron release from their anions.

$$C_6F_6^- \rightarrow C_6F_6 + e^- - 0.53\ \text{eV}, \tag{14}$$
$$C_6F_5Cl^- \rightarrow C_6F_5Cl + e^- - 0.75\ \text{eV}, \tag{15}$$
$$C_6F_5Br^- \rightarrow C_6F_5Br + e^- - 1.15\ \text{eV}, \tag{16}$$
$$C_6F_5CF_3^- \rightarrow C_6F_5CF_3 + e^- - 0.86\ \text{eV}. \tag{17}$$

On the other hand, the dissociation energies of $D(C_6F_5–X^-)$, $D(C_6F_5CF_2–F^-)$, and $D(F^-–C_6F_4CF_3)$, which are required for the formation of RgX* excimers, are as follows.

$$C_6F_6^- \rightarrow C_6F_5 + F^- - 2.16\ \text{eV}, \tag{18}$$
$$C_6F_5Cl^- \rightarrow C_6F_5 + Cl^- - 1.11\ \text{eV}, \tag{19}$$
$$C_6F_5Br^- \rightarrow C_6F_5 + Br^- - 1.19\ \text{eV}, \tag{20}$$
$$C_6F_5CF_3^- \rightarrow C_6F_5CF_2 + F^- - 3.05\ \text{eV}, \tag{21a}$$
$$C_6F_5CF_3^- \rightarrow C_6F_4CF_3 + F^- - 2.49\ \text{eV}. \tag{21b}$$

Since the electron affinity of $C_6F_5Br^-$ is largest among the four C_6F_5X reagents, an electron transfer from $C_6F_5X^-$ to Rg^+ is most unfavorable. On the other hand, the $D(C_6F_5–Br^-)$ value is smaller than those of $D(C_6F_5CF_2–F^-)$ and $D(F^-–C_6F_4CF_3)$. Therefore, it is expected that excimer formation via Br^- transfer occurs for $C_6F_5Br^-$. Since the $D(C_6F_5CF_2–F^-)$, and $D(F^-–C_6F_4CF_3)$ values are larger than those of other C_6F_5X reagents, F^- transfer is unfavorable for $C_6F_5CF_3^-$. On the other hand, the electron affinity of $C_6F_5CF_3$ is smaller than that of C_6F_5Br. Therefore, it is expected that neutralization reaction via an electron transfer is favorable exit channel for $C_6F_5CF_3^-$. These predictions are consistent with the experimental observations that excimer formation via Br^- transfer occurs for $C_6F_5Br^-$, as in the case of $C_6F_5Cl^-$,[16] whereas only neutralization reactions leading to low lying $Kr(5s[3/2]_1)$ and $Xe(6s[3/2]_1)$ states take place for $C_6F_5CF_3^-$. It was thus confirmed that electron affinities of target molecules and dissociation energies of $C_6F_5X^-$ leading to X^- play a significant role in the ion–ion recombination and neutralization reactions of Rg^+(Kr, Xe) with $C_6F_5Br^-$ and $C_6F_5CF_3^-$, as in the cases of $C_6F_6^-$ and $C_6F_5Cl^-$.[11,16]

4. Summary and Conclusion

The $Kr^+/C_6F_5Br^-$, $Xe^+/C_6F_5Br^-$, $Kr^+/C_6F_5CF_3^-$, and $Xe^+/C_6F_5CF_3^-$ ion–ion mutual recombination and neutralization reactions have been spectroscopically studied in the He flowing afterglow. The branching ratios of recombination and neutralization reactions were found to be 0.14:0.86, 1.00:0.00, 0.00:1.00, and 0.00:1.00 for the $Kr^+/C_6F_5Br^-$, $Xe^+/C_6F_5Br^-$, $Kr^+/C_6F_5CF_3^-$, and $Xe^+/C_6F_5CF_3^-$ reactions, respectively. These results suggested that the branching ratio between recombination reaction leading to RgX* excimer and neutralization reaction leading to Rg* atoms are different between $C_6F_5Br^-$ and $C_6F_5CF_3^-$. Results showed that Br^- transfer to form RgBr* excimers occurs for $C_6F_5Br^-$, whereas neutralization leading to Rg* through an electron transfer from $C_6F_5CF_3^-$ to Rg^+ is only product channel for $C_6F_5CF_3^-$. It was concluded that electron affinities of target molecules and dissociation energies of target molecular anions leading to X^- are important factors in determining the branching ratio between the recombination and neutralization channels in the ion–ion reactions of Rg^+(Kr, Xe) with $C_6F_5Br^-$ and $C_6F_5CF_3^-$, as in the cases of $C_6F_6^-$ and $C_6F_5Cl^-$ reported previously.[11,16]

Acknowledgments

The authors acknowledge Prof. Kenji Furuya of Kyushu University for his careful reading of our manuscript. This work has been supported by the Morino Foundation for molecular science (1992), the Iwatani Naoji Memorial Foundation (1993), and Showa Shell Sekiyu Foundation for environmental research (1995).

References

1) J. R. Peterson, W. H. Aberth, J. T. Moseley, and J. R. Sheridan, *Phys. Rev. A 3*, 1651 (1971).
2) J. T. Moseley, R. E. Olson, and J. R. Peterson, *Case Stud. At. Phys.*, 5, 1 (1975).
3) D. R. Bates, "*Case Studies in Atomic Physics*", Edited by E. W. McDaniel and M. R. C. McDowell, North Holland, Amsterdam, Vol. 4, p. 57 (1974).
4) D. Smith and M. J. Church, *Int. J. Mass Spectrom. Ion Phys.*, 19, 185 (1976).
5) M. J. Church and D. Smith, *J. Phys. D*, 11, 2199 (1978).
6) M. R. Flanney, *Adv. Atomic, Mol. Opt. Phys.*, 32, 117 (1994).
7) a) N. S. Shuman, T. M. Miller, R. Johnsen, and A. A. Viggiano, *J. Chem. Phys.*, 140, 044304 (2014). b) J. P. Wiens, N. S. Shuman, T. M. Miller, and A. A. Viggiano, *J. Chem. Phys.*, 144, 204309 (2016).
8) M. Zauner-Wieczorek, J. Curtius, and A. Kürten, *Atmos. Chem. Phys.*, 22, 12443 (2022).

9) M. Tsuji, M. Furusawa, and Y. Nishimura, *Chem. Phys. Lett.*, 166, 363 (1990).
10) M. Tsuji, M. Furusawa, H. Kouno, and Y. Nishimura, *J. Chem. Phys.*, 94, 4291 (1991).
11) M. Tsuji, H. Ishimi, and Y. Nishimura, *Chem. Lett.*, 25, 515 (1996).
12) M. Tsuji, *Trends Phys. Chem.*, 5, 25 (1995).
13) M. Tsuji, *Houshasenkagaku*, 62, 18 (1996).
14) M. Tsuji, M. Nakamura, and Y. Nishimura, *Chem. Lett.*, 26, 259 (1997).
15) M. Tsuji, M. Nakamura, Y. Nishimura, E. Oda, H. Oota, and M. Hisano, *J. Chem. Phys.*, 110, 2903 (1999).
16) M. Tsuji, H. Ishimi, K. Uto, and J.-I. Hayashi, *Eng. Sci. Rep., Kyushu Univ.*, 45, 7 (2023).
17) M. Tsuji, H. Ishimi, K. Uto, and J.-I. Hayashi, *Eng. Sci. Rep., Kyushu Univ.*, 45, 13 (2023).
18) A. L. Schmeltekopf and F. C. Fehsenfeld, *J. Chem. Phys.*, 53, 2000 (1970).
19) C. R. Herd, N. G. Adams, and D. Smith, *Int. J. Mass Spectrom. Ion Process.,* 87, 331 (1989).
20) F. J. Davis, R. N. Compton, and D. R. Nelson, *J. Chem. Phys.*, 59, 2324 (1973).
21) M. Tsuji, M. Ide, E. Oda, and Y. Nishimura, *J. Chem. Phys.*, 109, 3374 (1998).
22) C. E. Moore, "*Atomic Energy Levels*," U.S. GPO, Washington D.C., *Natl. Bur. Stand.* (U.S.) Circ. 467 (1949).
23) *Atomic Spectra Database*, *NIST Standard Reference Database*, 78, Ver. 5.9. Oct. (2021).
24) Y.-R. Luo, "*Bond Dissociation Energies*", in *CRC Handbook of Chemistry and Physics*, 81th Ed., CRC Press, Boca Raton (2000).
25) *NIST Chemistry WebBook*, *NIST Standard Reference Database*, Number 69 (2023) https://doi.org/10.18434/T4D303.
26) T. H. Dunning and P. J. Hay, *J. Chem. Phys.*, 69, 134 (1978).
27) P. J. Hay and T. H. Dunning, *J. Chem. Phys.*, 69, 2209 (1978).
28) M. T. Jones, T. D. Dreiling, D. W. Setser, and R. N. McDonald, *J. Phys. Chem.*, 89, 4501 (1985).
29) E. J. D. Vredenbregt, M. P. M. van Besouw, M. J. J. Vrakking, M. J. Mietus, C. E. P. Gerrits, and H. C. W. Beijerinck, *J. Chem. Phys.*, 98, 7903 (1993).
30) D. Zhong, D. W. Setser, R. Sobczynski, and W. Gadomski, *J. Chem. Phys.*, 105, 5020 (1996).
31) D. Zhong and D. W. Setser, *Chem. Phys. Lett.*, 207, 555 (1993).